

Magic Angle Chaotic Precession

Bernd Binder

Quanics, Salem, Germany,
Email: binder@quanics.com

in "Topics on Chaotic Systems: Selected Papers from CHAOS 2008 International Conference",
June 3-6, Chania, Crete, Greece, Editor Ch. Skiadas, Singapore, World Scientific (2008)

Abstract: This paper explores the properties of a precessing rotor or a coupled system of precessing rotors (gyroscopes), where a special chaotic behavior in the precession angle can be found if the change of rotor angular velocity is linearly coupled by (an)holonomy to the precession angular velocity and angle. The linear coupling provides for rolling cone paths and allows spinning up and controlling the rotor simply by forcing precession at special quantum magic precession angles. The geometric phase induced by the curved path of the rotor or external curvature and part of the coupling increases with precession angle. This leads to bifurcations in coupling strength resulting in chaotic precession. As an alternative to the $SO(3)$ matrix or quaternion representation the treatment of the three coupled rotations is here based on Euler's dynamical equations. First, the classical Magic Angle Precession (MAP) dynamics is realized by a geometric or mechanical condition (type I, transcendental solutions), where it can be experimentally demonstrated how MAP can "slave" angular degrees of freedom allowing the external control of high-frequent spin by slow oscillations. MAP is found in a commercial fitness device and is conceptually approached via Chua's electric circuit. Second, the quantum-gravitational MAP (type II, rational solutions) with discrete precession angles is analyzed on a deeper level requiring intrinsic curvature/relativistic effects adjusting holonomy to quantum numbers. Third, a macroscopic network of MAP elements is presented as a discrete-time recurrent neural network synchronizing to one common MAP I/II dynamics under special pairing and symmetry conditions (type III). In all three cases MAP can be treated as a time-discrete chaotic system with singularities given by the cosine map with several possible links to interesting applications on all scales.

Keywords: Chaotic precession, Spin-orbit coupling, Gyroscope, Magic Angle, Euler's Equations, $SO(3)$, Bifurcation, neural net, Chua, Berry, Hannay.

Introduction

Rotated spin systems like gyroscopes, precessing stars, rotating solids, superconductors, electromagnetic particles, or others are very interesting from many different points of view. Adding a few extra coupling or damping terms, which is typical for a real system, can lead to chaotic precession (like a dissipation induced instability or bifurcation [1]), where it is rather expensive to actively control chaotic motion to obtain the sufficient stability conditions at the equilibrium points even for relatively simple gyroscope systems [2]. Regarding this challenge and the broad spectrum of possible physical applications we focus on special conditions supporting fast auto-tuning and self-stabilization capabilities. In [3], [4], and [5] we have already identified a rather basic chaotic mechanism given by the cosine map, where the precession angle of rotated rotors can iterate towards an optimum. This

situation arises if the precession angle induced by an external or internal coupling becomes linearly related by a connection or (an)holonomy to the spin frequency shift of precession. Recently we were able to show [5] that the basic mechanism can be illustrated and experimented with well known commercial gyroscopes useful as a hand fitness device [6], but there is almost no published literature about its chaotic precession properties [7]. In this paper we will work out the dynamical equations of MAP. Comparing the classical transcendental recursion (type I) to the rational recursion (type II), there is some number theoretical evidence that type II requires relativistic degrees of freedom to realize quantum boundary conditions like quantum spin and precession numbers. Introducing the MAP spin network (type III) and some symmetry conditions the network behaves as one MAP element. The emerging differential or difference equations of precession provide for attracting and repelling “charge” singularities including broken symmetry, which has similarities to Chua’s Circuit. This helps to evaluate both, the classical and quantum-gravitational context of MAP.

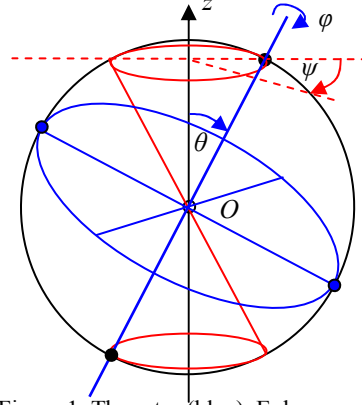


Figure 1. The rotor (blue), Euler angles, and precession cone (red).

1. Transcendental Spin-Orbit Recursion (MAP Type I)

It makes sense to separate MAP into irrational transcendental and rational solutions since rational quantum angles require some curvature assistance.

1.1. Kinematics, frequencies, and frequency shift in flat space

As an alternative to the $SO(3)$ matrix [4] or quaternion representation, we start with Euler’s dynamical equations [8],[9] based on angular relations. In Euler’s dynamical equations the angular velocity vector is expressed by three Euler angles describing the motion of the advancing frame with respect to the inertial frame. With mass points rotating and precessing on the sphere in flat space (which is a classical connection) the three Euler angles are, see fig.1:

1. θ , first Euler angle describing the precession tilt angle,
2. φ , second Euler angle describing the spin of the rotor axis,
3. ψ , third Euler angle describing the precession of the axis.

In Cartesian coordinates the rotor will precess around the z -axis. Assume that the rotor axis of a spherical rotating rotor precesses at frequency $\omega_\psi = d\psi/dt$. The temporal change of precession tilt called nutation is given by $\omega_\theta = d\theta/dt$. As a characteristics of precession the rotor rotating at frequency $\omega_\varphi = d\varphi/dt$ will experience a frequency shift ω_Δ , which is part of the invariant component ω_r given by the 3rd dynamical equation

$$\omega_r = \omega_\varphi + \omega_\Delta = \omega_\varphi + \omega_\psi \cos \theta, \quad (1)$$

(see [9] with notation $\omega_r = r$, $\omega_{p,q}^2 = p^2 + q^2$). With eq.(1) and according to [9] the kinetic energy T of the spherical symmetry is given by

$$T = \frac{1}{2} \omega_{p,q}^2 + \frac{1}{2} \omega_r^2 = \frac{1}{2} (\omega_\theta^2 + \omega_\psi^2 + \omega_\phi^2) + \omega_\Delta (\omega_r - \omega_\Delta). \quad (2)$$

From one Euler's equation, the other two follow by symmetry [9], where

$$\omega_{p,q}^2 = \omega_\theta^2 + \omega_\psi^2 \sin^2 \theta \quad \text{and} \quad \omega_\theta^2 + \omega_\psi^2 = \omega_{p,q}^2 + \omega_\Delta^2. \quad (3)$$

1.2. Geometric phase from (an)holonomy

Geometric phases naturally arise in the dynamics of coupled rigid bodies [10], [11], [1] (i.e. rolling on each other) or in curved space-time. Therefore, we will introduce $\bar{\theta}$ as a geometric phase or the Hannay anholonomy of the $U(1)$ bundle along the curve, where the 'parallel transported' spin vector (rotor axis) will come back after every loop or cyclic evolution with extra rotations equal to the curvature enclosed by the path [1], [11]. On the unit sphere with unit Gauss curvature the j extra rotations are given by

the spherical area Ω the precession axis sweeps, it is a curve integral within a precession period T providing for the difference between the total and dynamical phase

$$\Omega = T \omega_{\bar{\theta}} = 2\pi \frac{\omega_{\bar{\theta}}}{\omega_\psi} = 2\pi (1 - \cos \theta) = 2\bar{\theta} = \frac{2\pi j}{N}, \quad T = \frac{2\pi}{\omega_\psi}. \quad (4)$$

j and N are numbers characterizing the geometric phase shift induced by external accelerations, fields, or relativistic effects (by motion or curvature). Dividing the precession period into M invariant units, the 3rd dynamical invariant ω_r is M -times the precession frequency

$$\omega_r = \omega_\psi M. \quad (5)$$

The special case $M = 1$ corresponds to $\omega_r = \omega_\psi$, $|\theta| = \pi/2$, and $j = 1$, with $\omega_r = N\omega_1$ and $\omega_{\bar{\theta}} = \omega_1 = \omega_\phi$, see figs.1 and 2.

1.3. The coupling parameter α

According to eqs.(1)-(5) the dynamical phase or total phase minus geometric phase can be found in the z -axis with $z = \cos \theta$ from the tilt/precession angle θ in terms of j and N , see fig.2, resulting in a relative frequency shift given by the transcendental number (the rational case will be MAP type II)

$$\frac{\omega_\Delta}{\omega_\psi} = \cos \theta = \frac{N-j}{N}, \quad 0 < j < N. \quad (6)$$

According to eqs.(4) and (6) the coupling and corresponding frequency shift

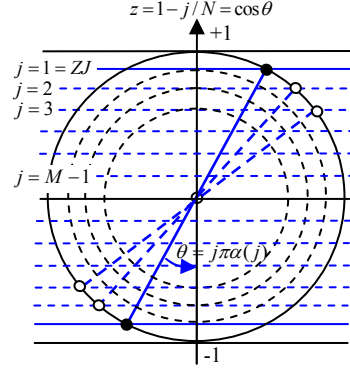


Figure 2. Geometric phases and precession with $|j/N| > 0$. Here $M=7$.

can be interpreted as a geometric phase changing the precession frequency, where the product $\omega_\Delta \omega_{\bar{\theta}}$ is linearly related to the nutation frequency ω_θ

$$\omega_\Delta = \omega_\psi - \omega_{\bar{\theta}} = \omega_r - \omega_\phi, \quad \omega_\theta \omega_\psi = \omega_\Delta \omega_{\bar{\theta}}. \quad (7)$$

The coupling parameter describing the shift and dynamical phase evolution within one precession loop can be defined according to eqs.(4-7) by

$$\alpha = \frac{\cos \theta}{M} = \frac{\omega_\Delta}{\omega_r} = \frac{\omega_\psi - \omega_{\bar{\theta}}}{\omega_r} = \frac{1}{M} - \frac{\omega_{\bar{\theta}}}{\omega_r} = \frac{N-j}{NM}. \quad (8)$$

Eq.(8) can characterize the fine structure of spin-orbit coupling [3]. With eq.(2) the coupling constant $|\alpha| > 0$ leads to a shift $|\omega_\Delta| > 0$, $\alpha = 0$ corresponds either to $\omega_\psi = 0$ or $|\theta| = \pi/2$, see the red curve in fig.3. Assuming positive frequencies and $\omega_1 = \omega_{\bar{\theta}} (j=1)$ we get with eqs.(1)-(8) $\omega_r > \omega_\phi > \omega_\psi > \omega_\Delta > \omega_{\bar{\theta}} > \omega_\theta$, where

$$\omega_1 = \frac{\omega_r}{MN} = \frac{\omega_\phi}{N(M-1)+j} = \frac{\omega_\psi}{N} = \frac{\omega_\Delta}{N-j} = \frac{\omega_{\bar{\theta}}}{j} = \frac{N\omega_\theta}{j(N-j)}. \quad (9)$$

1.4. The geometric feedback condition leading to chaotic precession

As a criterion for precessional coupling, the precession angle subject to dissipation will nutate according to eq.(7). The amplitude of nutation will decrease during the dissipation process. The corresponding angular contraction (Jacobian flow) and response in T will be given by one rotator loop out of M

$$-\omega_1 \frac{\theta}{\pi} = \frac{1}{M} \frac{d\theta}{dt} = \frac{\omega_\theta}{M} \frac{\cos \theta}{M}. \quad (10)$$

Since the geometric phase $\bar{\theta}_t$ is evaluated within one discrete precession

loop period, the precession angle for a new precession period T_{t+1} at time $t+1$ is determined by the dynamics and precession angle of the previous period T_t at time t providing with eq.(10) for a time-discrete coupling $\alpha_t(\theta_t)$ and angle

$$\theta_{t+1} = \pi j_t \alpha_t(\theta_t) = \frac{\pi}{M} \frac{j_t}{N_t} (N_t - j_t) = \pi j_t \frac{\omega_{\Delta,t}}{\omega_{r,t}}. \quad (11)$$

Because of the recursive relation between geometric phase contribution $\bar{\theta}_t$ and the precession angle in eq.(11) we can expect chaotic precession. With a dimensionless z -variable according to fig.2 and the z -Phase $\tilde{\theta}_t$

$$z_{t+1} \propto \theta_t(z_t), \quad z_t = 1 - \frac{j_t}{N_t} = 1 - \frac{\bar{\theta}_t}{\pi} = \frac{\tilde{\theta}_t}{\pi}, \quad (12)$$

the number j of geometric extra loops in eq.(11) become in the stable case the fixed points $j = N(1 - M\alpha)$ of a logistic map, whereas $\tilde{\theta}_{t+1}$ or the precession

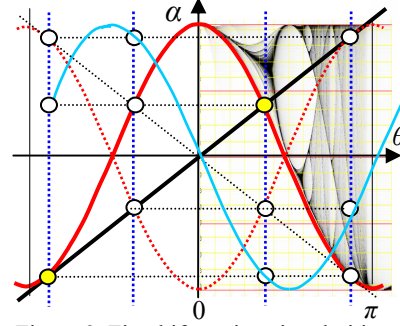


Figure 3. First bifurcation singularities (yellow) at $\theta \tan \theta = 1, \theta = \pm 0.8603336\dots$

angle can be iteratively computed from a time-discrete cosine chaotic map showing bifurcations (see figs.3,5) with transcendental solution

$$\tilde{\theta}_{i+1} = \pi \cos \tilde{\theta}_i, \quad \theta_{i+1} M = j \pi \cos \theta_i. \quad (13)$$

With the precession angle linearly related to the spinning phase/frequency offset induced by precession we have the MAP feedback situation recursively adjusting or auto-tuning the precession angle and frequency to the external acceleration source eventually leading to coupling anomalies [14].

1.5. Approaching the dynamics of MAP with Chua's Circuit

To model the chaotic precession / nutation dynamics in eqs.(10)-(13) we can refer to a well known and rather simple system of coupled differential equations, where the angular /phase space occupation density and flow of the attractor can be simulated and visualized, see fig.4 (the time discrete simulation uses the difference equation version)

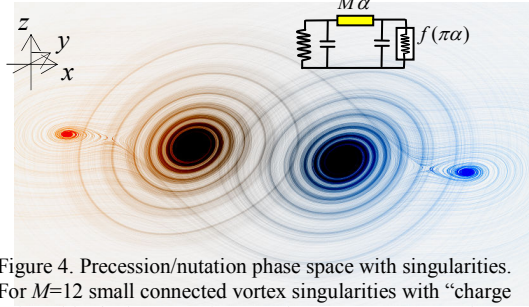


Figure 4. Precession/nutation phase space with singularities. For $M=12$ small connected vortex singularities with “charge pairs” (blue/red) appear for $j>10$, here $j=12$, see (14). The yellow conductive/coupling term provides for dissipation.

$$\begin{aligned} dz &= \omega_v M (y - z) dt + \omega_v f(y - z) dt, \\ dy &= \omega_v x dt - \omega_v M (y - z) dt, \\ dx &= -\omega_v y dt, \end{aligned} \quad (14)$$

with $\pi x = \tilde{\theta}$, $\pi j \alpha = \theta = j(y - z)$, $f(y - z) = \pm \pi \cos[j(y - z)]$.

This is a form of Chua's electronic circuit, a well known and real-world example showing chaotic dynamics [12]. MAP can be approached and illustrated if we take the precession angle as the voltage term (showing Coulomb type “charge” and dipole effects) and the rotor spin as the electric current (showing magnetic monopole [8] and dipole effects). Both systems have 3 degrees of freedom (two voltage y, z , one current x) and 3 energy storage elements (two capacitors and one inductivity as the rotor angular momentum setting the timescale $\omega_r = \omega_v M$). In both cases a linear oscillator (precession in MAP) is coupled to a nonlinear element (anholonomy in MAP). The nonlinear element $f(\theta / j)$ responsible for chaos and bifurcation is driven by precession $\theta = j(y - z)$, where the geometric coupling current is delivered by the conductivity term $M(y - z)$ providing for j missing or extra loops (monopoles with charge M). Both systems show vortex singularities at points where the linear coupling current equals the nonlinear current. Asymmetric pairs of attracting vortex singularities show $|j / M| \geq 0.839801$,

see figs.4-6. With eqs.(10)-(13) we get near the vortex singularities ($dx/dt = dy/dt = 0$) a spiraling in plane $j\theta = M\theta$, the MAP condition can be found in eq.(14) from $dz/dt = d\bar{\theta}/dt = 0$, nutation can be assigned to $d\theta/dt \neq 0$. The first bifurcation is the second contact or intersection (singularity) of the nonlinear $\cos \theta$ and the linear coupling term proportional to θ , see fig.3, the tangent to the cosine function (slope is given by the sine function) at $\theta \tan \theta = 1$ with $\theta = 0.5\pi \cdot 0.8603336\dots$ and $j/M \sim 0.839801\dots$

1.6. Powerball example

Based on this analysis it was recently proposed [5] that the MAP type I conditions are present in the ‘‘Powerball’’ system [6], [7]. The function of this device is based on a mechanical

gear-type coupling between precession and spin frequency, see eq.(11). The rolling axis diameter at the end of the rotor shaft (#28 in [6]) is usually about 2 mm, the diameter of the groove (#24) or bearing ring element (#30) about 60 mm providing for $N \sim 30 = 60\text{mm}/2\text{mm}$ that counts how often the spin axis has to roll in the circular bearing to turn its axis by

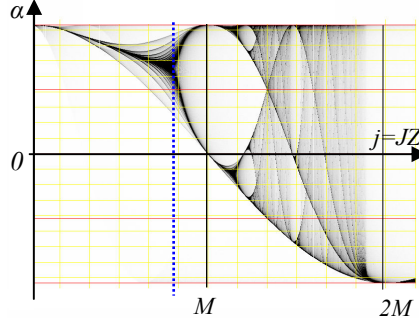


Figure 5. MAP bifurcation diagram [3],[4]. Smearing effects due to phase fluctuations.

360° with precession angle $\theta = \pi/2$, where $\omega_\Delta = \omega_\psi$. A wobbling by the hand introduces (an)holonomy and a shift by ω_θ , see eqs.(6)-(10). The MAP angle is given by $\theta = \arccos[(N - j)/N]$, see fig.2, a Powerball with $N \sim 30$, $M \sim 12$ and $j = 1$ has $\theta(j = 1) \sim 15^\circ$, bifurcation starts near $j = JZ \sim 10$ or 75° .

2. Polynomial Quantum-Gravitational Connection (Type II)

Type I provides according to eq.(13) transcendental solutions, but curvature (by relativity or external accelerations) can support periodicity with rational or polynomial solutions which look like closed loop rolling cone paths. Under the Lorentz rotation group $SO(3)$ rolling cone paths can describe anholonomy and precession (see e.g. [1],[3],[4],[11]) while providing for special periodicity conditions. In this case we get curves of constant precession (Darboux) in the Frenet description from the periodicity condition in the $SO(3)$ rotation matrix representation in [4], characterizing the cone rotation by $\cos(2\pi N \cos \theta) = \cos[2\pi(N - j)] = 1$ related to the cone geometry with $N \in [1, 2, \dots] > j \in [1/2, 1, 3/2, \dots]$ in a single-valued monochromatic loop.

2.1. Tschebyscheff polynomials of the first kind

With integral $N, M, 2j$ we get periodicity and monochromatic precession, where eq.(11) provides for the closed loop conditions current condition

$$\cos \theta = \cos(n\theta), \quad n = MN / j. \tag{15}$$

Eq.(15) provides for a finite order Tschebyscheff polynomial solution $T_n(x)$

$$T_n(x) = \cos[n \arccos(x)], \quad \frac{d^2 T_n}{d\theta^2} + n^2 T_n = 0, \quad (16)$$

representing the MAP type II precession and geometric phase condition relating the first polynomial $T_1(x) = x$ and linear tilt/precession term as an amplitude/phase condition to a higher polynomial

$$T_n(x) = T_1(x) = x, \quad \text{where } T_{n+1}(x) = 2xT_n(x) - T_{n-1}(x). \quad (17)$$

The polynomial can be written as a sum or a product,

$$T_n(x) = \sum_{i=0}^{\text{Floor}(n/2)} \binom{n}{2i} x^{n-2i} (x^2-1)^i = 2^{n-1} \prod_{k=1}^n \left\{ x - \cos \left[\frac{(2k-1)\pi}{2n} \right] \right\}, \quad (18)$$

where the zeros are with eqs.(11) and (18) at $k = (N-j) + \frac{1}{2}$. Mapping the x -current to a 2-dimensional y, z -precession in circular coordinates (voltage projection in Chua's circuit we get a closed loop nutation pattern, see fig.6,

$$T_n(z = \cos \theta, y = \sin \theta) = \sum_{i=0}^{\text{Floor}(n/2)} \binom{n}{2i} z^{n-2i} (-y^2)^i. \quad (19)$$

With the phase advance proportional to frequency at a given time period, the Chebyshev relations above provide for a frequency filter connecting the 1- d current and the 2- d closed loop space-time holonomy and dynamics.

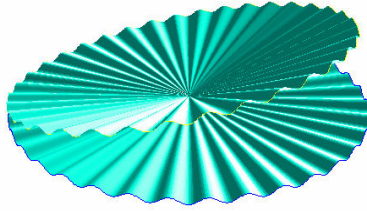


Figure 6. Closed modulated surfaces [4] by 2d Tschebyscheff polynomials in (19).

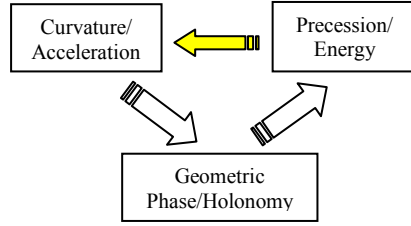


Figure 7. MAP recursive chaotic relation in space-time adjusting (an)holonomy.

2.2. MAP and Relativity

In General Relativity (an)holonomy can be directly related to curvature, see i.e. [1],[10],[11],[13], where the precession induced by curvature and/or torsion angle is directly given by the coupling strength. W. de Sitter was the first who predicted geodetic precession in curved space-time [13], where the gyroscope will be carried by parallel transport along the path of free fall. Regarding MAP one could argue on a number theoretical level (15)-(19) that it is more economic to avoid transcendental and prefer rational or polynomial values based on (an)holonomy adjusted by recursion to periodicity, see fig.7. This would mean that there could be a natural preference for curved space-time and anholonomy supporting closed loop conditions on scales comparable to the self-coherence length, which is large in superconductors. MAP is expected to occur on all scales, see the table of candidates [14]. If we apply MAP as a coupling condition on the cosmic scale, the scale below the

co-expanding unit scale appears to be contracting relative to the expanding unit scale, which is the inversion scale [15].

3. MAP Spin-Network Connection (Type III)

Precession dynamics including coupling according to eq.(14) can lead to synchronization in a network of coupled spins J_i . A “charged” discrete-time recurrent neural network can be found with a number Z of MAP elements connected by matrix coefficients ω_j , if the resulting precession angle is the sum of all weighted components of the previous stage

$$\theta_{j,t+1} = \pi J_j \cos \left(\sum_{i=0, i \neq j}^{Z-1} \omega_{ij} \theta_{i,t} \right), \quad (20)$$

where the sin/cosine transfer function is obviously exotic according to [16]. Defining a mean MAP by the time-discrete weighted sum of MAP elements

$$\theta_{is,t+1} = \sum_{j=0}^{Z-1} \omega_j \theta_{j,t+1} = \sum_{j=0, j \neq i}^{Z-1} \omega_j \theta_{j,t+1} + \omega_{ii} \theta_{i,t} = \pi J_i \sum_{j=0}^{Z-1} \omega_{ij} \cos(\theta_{is,t} - \omega_{ij} \theta_{j,t}), \quad (21)$$

analytical solutions requiring synchronization can be obtained with a simple homogeneous interaction model. With coupling coefficients $\omega_j = M^{-1}$ supporting eq.(10) as the dynamic coupling strength, the global mean system $\theta_{is,t+1}$ behaves like a single MAP element in eq.(13) with charge Z

$$\theta_{is,t+1} = \frac{\pi J_i}{M} \sum_{j=0}^{Z-1} \cos(\theta_{js,t} - \omega_{jj} \theta_{j,t}) = \pi \frac{J_i Z}{M} \cos(\theta_{is,t}). \quad (22)$$

This requires some symmetry conditions in precession dynamics, which can be achieved by a pair wise cancellation of cosine terms in the sum of eq.(22) with precession pairs $\cos \theta_1 + \cos \theta_2 = 0$ or by a symmetric distribution of local MAP angles around the mean $\theta_{is,t}$ with $\omega_{jj} \theta_{j,t} = \pi j / (Z-1)$.

Since $SU(2)$ is the spin double cover of the group $SO(3)$, MAP could be relevant to relativistic quantum systems like the spin-orbit Eigenstates of a relativistic electron and also to “charged” spin network systems in the solid or nuclear range [3]. Free fall precession in curved space (with Berry-Hannay connection) can generate at the center a magnetic monopole if the blue point in fig.1 is a charge [9]. Magnetic monopoles are field configurations that arise naturally in gauge field theories, even at the classical level. A monopole requires the non-integrability of the phase of the wave function leading to a singularity. In MAP these are the singularities, where the nonlinear cosine equals the linear extra-precession term (see figs.3-5). With $j = JZ$, charge Z , spin J , and MJ the Dirac monopole charge quantum number, MAP type III could be related to the nature of the electromagnetic field and the vector potential. $M=137$, $J=0.5$, $Z=2$ (Cooper pairs) could be relevant to superconductivity with Berry’s phase part of the fine structure in the Josephson effect. The first bifurcation for a closed loop spin-network system (heavy nuclear particle) would occur near $Z=115.05275\dots$, see figs.3,5. Strong monopoles could be generated by MAP superconductor discs [3],[4].

4. Conclusions

It was found that a time-discrete chaotic system given by the cosine map can model a special recursive spin-spin coupling situation, where the precession angle of a rotating rotor is linearly related to the frequency shift induced by precession. The frequency or energy shift (precession forces) couple back to the internal or external acceleration (equivalent to a curvature) affecting holonomy and exciting j extra rotor loops with monopole charge M . If we allow for this chaotic feedback, the systems can auto-tune to an external precession starting bifurcations at $j/M > 0.84$ in experiments and simulation, see the Powerball device [6] and Chua's circuit approach [12]. The MAP dynamics carries the symmetry of the Lorentz group $SO(3)$, where degrees of freedom get frozen to $SO(2)$ or $U(1)$. The geometric phase shows a $2d$ to $1d$ mapping, where quantum-relativistic type II precession angles with space-time bending effects could generate closed loop periodicity conditions are supported by the Tschebyscheff polynomials. With synergetic effects given by a neural-type recursive network based on coupled MAP elements, a strong long range spin-network synchronization dynamics should be possible.

References

- [1] J. E. Marsden, T. Ratiu, Introduction to Mechanics and Symmetry, *Texts in Applied Mathematics* vol. 17, Springer-Verlag, 1994.
- [2] H. K. Chen, Chaos and Chaos Synchronization, *J. Sound Vib.* 255(4): 719-740, 2002.
- [3] B. Binder, "Geometric Phase Locked in Fine Structure" in *Iterative Coupling and Balancing Currents*, e-Book, ISBN:3-00-010972-2, 2003; "Berry's Phase and Fine Structure", <http://philsci-archive.pitt.edu/archive/00000682/>, updated at www.quanics.com/alfa137MN6.pdf, 2002, accessed 01.09.2002.
- [4] B. Binder, Magic Angle Precession, *AIP Conf. Proc.* 969: 1103-1110, 2008.
- [5] B. Binder, Magic Angle Precession at STAIF 2008, *Quanics Presentation notes*, www.quanics.com/MAPTalk20080214.pdf, 2008, accessed 14.02.2008.
- [6] L.A. Mishler, Gyroscopic Device, *United States Patent* 3,726,146, 1973.
- [7] P.G. Heyda, Roller ball dynamics Revisited, *Am. J. Phys.* 70: 1049-51, 2002.
- [8] W. F. Osgood, On the Gyroscope, *Transactions of the American Mathematical Society*, 23(3): 240-264, 1922.
- [9] W. F. Osgood, *Mechanics*, MacMillan, New York, 1937.
- [10] F. Wilczek, A. Zee, Appearance of Gauge Structure in Simple Dynamical Systems, *Phys. Rev. Lett.* 52: 2111, 1984.
- [11] A. Ishlinskii, Mechanics of Special Gyroscopic Systems, *Izd. AN USSR*, Kiev, 1952.
- [12] T. Matsumoto, L.O. Chua, M. Kumoro, The Double Scroll., *IEEE Transaction on Circuits and Systems*; CAS-32(8): 798-818, 1985.
- [13] C. Misner, K. Thorne, J. Wheeler, *Gravitation*, Freeman, 1973.
- [14] B. Binder, www.quanics.com/MAP_TableProcesses.pdf, accessed 12.03.2008.
- [15] B. Binder, Friedmann Propulsion in an Flat Holographic Universe, *AIP Conf. Proc.* 969: 1146-1153, 2008.
- [16] W. Duch, N. Jankowski, Transfer Functions: Hidden Possibilities for Better Neural Networks, 9th European Symposium on Artificial Neural Networks, 81-94, 2001.